Extended Abstracts of the 2007 International Conference on Solid State Devices and Materials, Tsukuba, 2007, pp. 786-787

F-6-3

Compositionally Bi-layered Formation of Interfacial Voids in a Porous Anodic Alumina Template Directly Formed on Si

Hong-Seok Seo[1], Yang-Gyoo Jung[1], Sang-Won Jee[1], Jun Mo Yang[2] and Jung-Ho Lee[1, *]

[1] Department of Materials and Chemical Engineering, Hanyang University, Ansan, Kyounggi 426-791, Korea
Phone: +82-31-400-5278 *E-mail: jungho@hanyang.ac.kr
[2] National Nanofab Center, Daejon 305-806, Korea

1. Introduction

In contrast to the conventional anodization of aluminum foils [1-3], one notable feature that has recently been reported [4-7] in the fabrication of wafer-level PAA templates is the formation of interfacial voids with inverted barrier morphology. A comprehensive understanding of the key factors affecting void formation is of great importance if one is to specifically tailor the void profiles along with the inverted shape of the barrier layers. Unfortunately, the origin of void formation and the relevance of the inversion behavior of the barrier morphology remains poorly understood. Here, we show that the formation of interfacial voids consists of multiple stages, such as the substrate touching a barrier layer, curvature inversion of the barrier layer by void nucleation, dendritic branching from the pore bottom edges, the formation of channels between pore bottoms and voids, and a local oxidation of silicon (LOCOS) [8] by electrolytes infiltrating through the channels. The compositionally bi-layered morphology of interfacial voids was found to be a thin Al-rich layer surrounded with the Al-deficient oxide.

2. Experiments

A 1- μm -thick aluminum film was deposited on n-type, <100> 4-in. silicon wafers using thermal evaporation. A two-step anodization process was used to fabricate the PAA templates on the Si substrates. As an electrolyte, diluted oxalic acid (0.3 M) was chosen for the anodization process under constant bias of 60 V at 5 °C . After the first anodization step, the alumina film was removed using a solution of 6.4 vol.-% H3PO4 and 19 g/L CrO3 acid at 60 °C for 10 min.

3. Results and Discussion

Fig. 1 depicts the process flow of void formation with curvature inversion of the barrier membrane. Further anodization of the Al metals remained when the barrier layer touched the substrate creates additional stress at the interfacial region between the pore bottoms and the substrate for alumina transformation. In contrast to the anodization of Al foils, the residual Al, firmly attached to the rigid substrate, can not accommodate the stresses by volume expansion without interfacial restructuring to create the necessary additional space.

The driving force for void nucleation is the stress pushing the substrate downwards owing to a laterally confined structure that is tightly attached to a rigid substrate. Correspondingly, upward stresses (fig. 1(b) and (c)) are concentrated on the bottom side of each pore array, which then makes the curvature of the pore bottoms dull. Since the edge profile of pore bottoms becomes angular while the pore bottoms flatten, the electric field for anodization is likely to be locally concentrated. As a result, a dendritic branching behavior appeared from the edges of the pore bottoms (fig. 1(c)). The blunt curvature of the barrier layer is rapidly inverted based on a combination of the downward etching of pore edges and the stress. During the alumina transformation of residual Al metals, the upward stress acting on the pore bottoms increases due to void growth, but the inversion behavior of the barrier layer allows the barrier layer to be farther away from the substrate, which alleviates the stress burden while the barrier layer becomes thinner upon further anodizing. In fact, the distance between the center of the pore bottoms and the substrate is found to be almost similar (fig. 1, $y \cong y'$).

Horizontal and vertical line scans of nanoprobe EDS (fig. 2(b) and (c)) revealed that the voids were surrounded with a thin Al-rich layer. The compositional morphology which surrounded the voids reflected a bi-layered structure that consisted of thin (1~5 nm) Al-rich and thick (~20 nm) Al-poor regions. To further clarify this feature, we attempted the two-dimensional reconstruction (fig. 2(d)).

The Al concentration in the Al-rich layer was found to decrease from the void top to the bottom edges of voids. This feature could be understood based upon the kinetic competition between the void formation and the alumina transformation. The alumina film located just underneath the pore arrays is not generally given enough time for anodization because it becomes detached from the substrate for void formation. Given that the Al requires rather longer time for alumina transformation, the alumina film underneath the pore arrays is likely detached from the substrate as a form of Al-rich layer. Further transformation of Al-rich layer is allowed only for the bottom edges of voids in direct contact with the substrate (fig. 3). Finally, the Al-rich layer, which is electrically isolated from the substrate, remains on the top regions of voids in spite of the over-anodization. Therefore, the bi-layered feature we observed is the thin Al-rich layer surrounded with the Al-deficient oxide. The presence of a thin Al-rich layer, which is electrically disconnected from the substrate, strongly implies that the interfacial voids were formed physically.

Further anodization after dendritic branching from the pore bottom edges resulted in the formation of channels between the pore bottoms and the top-side of voids, which allows the infiltration of electrolytes into the voids. Then, the silicon surfaces inside the voids were oxidized by electrolytes (fig. 4). This feature has been named a “bird’s beak (BB)” [8]. The BB formation, in our case, was chemically driven by electrolytes.

4. Conclusions

In summary, we have explained the process of void formation in an alumina film anodized on a Si substrate. EDS analysis revealed that the voids were surrounded with a typical bi-layer structure that consisted of thin, Al-rich and thick, Al-poor regions.

References

[1] K. Nielsch, J. Choi, K. Schwirn, R. B. Wehrspohn and U. Gösele, Nano Lett. **2** (2002) 677.

[2] H. Masuda and K. Fukuda, Science **268** (1995) 1466.

[3] H. Masuda, H. Yamada, M. Satoh, H. Asoh, M. Nakao and T. Tamamura, Appl. Phys. Lett. **71** (1997) 2770.

[4] M. Kokonou, A. G. Nassiopoulou and K. P. Giannakopoulos, Nanotechnology, **16** (2005) 103.

[5] O. Rabin, P. R. Herz, Y. M. Lin, A. I. Akinwande, S. B. Cronin and M. S. Dresselhaus, Adv. Funct. Mater. **13** (2003) 631.

[6] D. Crouse, Y. H. Lo, A. E. Miller and M Crouse, Appl. Phys. Lett. **76** (200) 49.

[7] M. T. Wu, I. C. Leu and M. H. Hon, J. Mater. Res. **19** (2004) 888.

[8] S. Wolf, *Silicon Processing for the VLSI Era*, **Vol. 2**: Process Integration, Lattice Press: Sunset Beach, California (1990) pp.20.

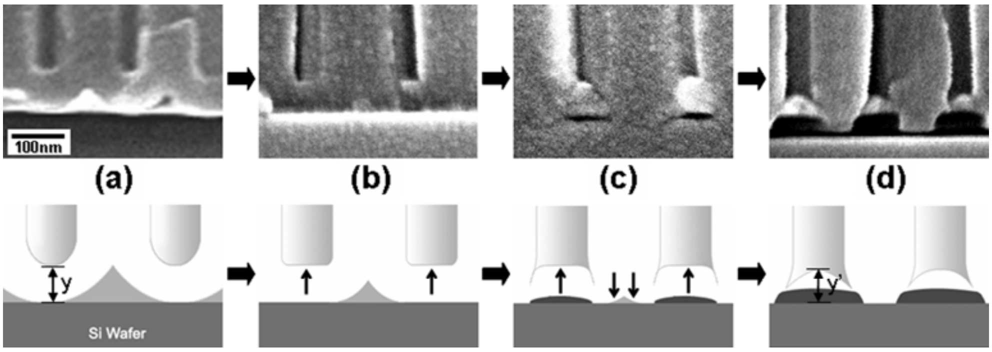

Fig. 1 Cross-sectional scanning electron microscopy (SEM) images (top) and a cartoon schematic (bottom) showing the process flow of void formation: (a) residual Al is shown, (b) stresses make the pore bottoms dull, (c) stresses can be released by void nucleation, and (d) the edge profile of pore bottoms becomes angular. The stress directions are displayed by arrows.

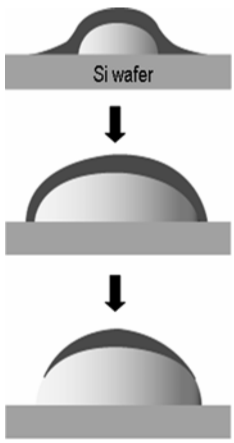

Fig. 3 A cartoon schematic explaining the formation process of the Al-rich alumina(black): (Top) the Al-rich layer film located just underneath the pore arrays; (Center) further anodization of Al-rich layer is allowed only for the bottom edges of voids; (Bottom) finally, the Al-rich remains on the top regions of voids

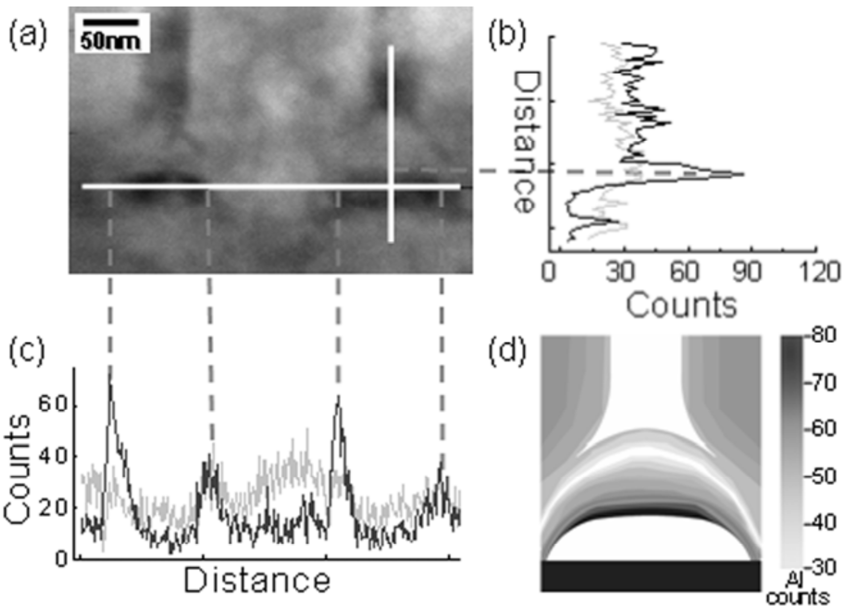

Fig. 2 Transmission electron microscopy (TEM) image (a) and line scans (b) and (c) of nanoprobe EDS; aluminum (black) and oxygen (gray), and (d) two-dimensional reconstruction of Al concentration.

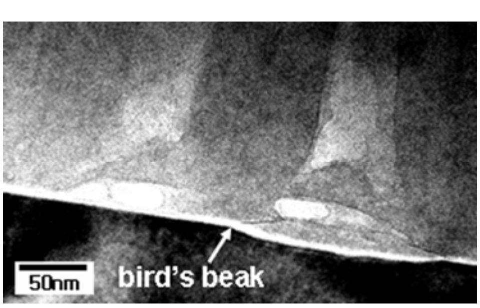

Fig. 4 TEM image showing a bird's beak formed by silicon oxidation.